Curcumin-encapsulated hydrophilic gelatin nanoparticle to stabilize fish oil-loaded Pickering emulsion

Guangyi Kan [a,b], Ye Zi [a,b], Li Li [a,b], Huan Gong [a,b], Jiawei Peng [a,b], Xichang Wang [a,*], Jian Zhong [a,b,*]

[a] National R&D Branch Center for Freshwater Aquatic Products Processing Technology (Shanghai), Integrated Scientific Research Base on Comprehensive Utilization Technology for By-Products of Aquatic Product Processing, Ministry of Agriculture and Rural Affairs of the People's Republic of China, Shanghai Engineering Research Center of Aquatic-Product Processing and Preservation, College of Food Science & Technology, Shanghai Ocean University, Shanghai 201306, China
[b] Xinhua Hospital, Shanghai Institute for Pediatric Research, Shanghai Key Laboratory of Pediatric Gastroenterology and Nutrition, Shanghai Jiao Tong University School of Medicine, Shanghai 200092, China

ABSTRACT

Herein, pH-cycle method was explored to prepare curcumin-encapsulated hydrophilic bovine bone gelatin (BBG/Cur) nanoparticle and then the obtained nanoparticle was applied to stabilize fish oil-loaded Pickering emulsion. The nanoparticle had a high encapsulation efficiency (93.9 ± 0.5 %) and loading capacity (9.4 ± 0.1 %) for curcumin. The nanoparticle-stabilized emulsion had higher emulsifying activity index (25.1 ± 0.9 m^2/g) and lower emulsifying stability index (161.5 ± 18.8 min) than BBG-stabilized emulsion. The pH affected the initial droplet sizes and creaming index values of the Pickering emulsions: pH 11.0 < pH 5.0 ≈ pH 7.0 ≈ pH 9.0 < pH 3.0. Curcumin provided obvious antioxidant effect for the emulsions, which was also dependent on pH. The work suggested pH-cycle method could be used to prepare hydrophobic antioxidant-encapsulated hydrophilic protein nanoparticle. It also provided basic information on the development of protein nanoparticles for Pickering emulsion stabilization.

Introduction

Protein nanoparticles have attracted more and more attentions in the field of colloid science for the preparation of oil-in-water Pickering emulsions (Zhang, Xu, et al., 2021). Many physical preparation methods have been developed for the preparation and application of protein nanoparticles because of their superiorities (e.g., simple operation and excellent safety for food application) (Huang, et al., 2019). pH-cycle (named as pH-shifting or pH-driven) method is an emerging physical preparation method for the preparation of hydrophobic protein nanoparticles by adjusting the neutral pH to extremely alkaline or acidic pH and then back to neutral pH (Jiang, Wang & Xiong, 2018; Sun, Gao & Zhong, 2018; Fu, et al., 2020). However, to the best of our knowledge, pH-cycle method has not been used to prepare nanoparticles of hydrophilic proteins, which limited the wide application of pH-cycle method

for protein research.

Gelatins are obtained by hydrolysis of collagens and are widely-used natural hydrophilic macromolecules in the fields of food, cosmetics, medicine, and drug delivery (Wu, et al., 2020; Alipal, et al., 2021). Due to their unique properties in rheology, emulsifying, and gel properties (Duconseille, Astruc, Quintana, Meersman & Sante-Lhoutellier, 2015), gelatins have been broadly applied as food additives (e.g., foaming, emulsifying, and wetting agents) in food (e.g., dairy products, baked goods) (Karim & Bhat, 2009). Many physical and chemical modification methods have been applied to develop gelatin nanoparticles to increase the emulsifying properties (Zhang, Xu et al., 2020). For example, two-step desolvation aldehyde crosslinking modification method could be applied to form gelatin nanoparticles to stabilize emulsions (Ding, et al., 2019, 2020b). At the same middle gelatin concentrations, the diameters of gelatin nanoparticles were generally larger than the thickness of

uncrosslinked gelatin layer at the oil–water interface, and therefore, some gaps might be present between gelatin nanoparticles in the oil––water interfaces of Pickering emulsions. So, Pickering emulsions stabilized by gelatin nanoparticles had lower creaming stability than traditional emulsions stabilized by uncrosslinked gelatin molecules at the middle gelatin concentrations (Ding, et al., 2020b). In addition, a self-assembly method was applied to prepare chitosan/gelatin nanoparticle to increase long-term emulsion stability (Wang & Heuzey, 2016). However, physical modification methods have not been widely used to prepare gelatin nanoparticles for emulsion stabilization.

Curcumin is a hydrophobic polyphenol nutrient with potential anti-inflammatory, anticancer and antioxidant activities (Zhang, Li, et al., 2021; Cao, et al., 2022). It was generally encapsulated in the oil phase of emulsion to enhance its stability, antioxidant activity, delivery, and bioaccessibility (Shah, Zhang, Li & Li, 2016; Lei, et al., 2022; Saffarionpour & Diosady, 2022). The combination of hydrophobic curcumin with hydrophilic gelatin might increase the emulsifying properties of gelatin and provide a certain antioxidant effect for the emulsions. However, curcumin-encapsulated hydrophilic gelatin nanoparticle has not been developed for the stabilization of Pickering emulsions.

The aim of this study was to develop curcumin-encapsulated hydrophilic gelatin nanoparticle for the stabilization of fish oil-loaded Pickering emulsion. Bovine bone gelatin (BBG) was selected as a representative gelatin material. Firstly, BBG/Cur nanoparticle was prepared by a pH-cycle method and characterized. Secondly, fish oil-loaded emulsions stabilized by BBG/Cur nanoparticle were prepared and characterized at different solution pH. Thirdly, the emulsifying parameters of BBG/Cur nanoparticle were analyzed. Finally, the storage stability of the emulsions stabilized with BBG/Cur nanoparticle at different pH was studied.

Materials and methods

Reagents

BBG (~240 g bloom, type B) was bought from Aladdin Industrial Corporation (Shanghai, China). Curcumin (analytical grade, stored at −20 °C) was bought from Shanghai Macklin Biotechnology Co., ltd. (Shanghai, China). All other reagents were bought from Sinopharm Chemical Reagent Co., ltd. (Shanghai, China).

Preparation of BBG/Cur nanoparticle

BBG/Cur nanoparticle was prepared by a pH-cycle method (Zhan et al., 2020). Briefly, 10 mg/mL BBG solution was prepared by swelling 1.0 g of BBG into 100 mL of ultrapure water for 10 min and then incubating it at 45 °C for 30 min with stirring using glass rod. The pH was adjusted to 12.0 using 4 mol/L NaOH. After magnetically stirring (400 rpm) for 5 min, 0.1 g of curcumin was added and then the mixture was continuously stirred for 30 min. Subsequently, the solution pH was adjusted to 7.0 by 1 mol/L HCl to form BBG/Cur nanoparticles. The solution was centrifuged at 1375 × g for 30 min to deposit large precipitates. The supernatant was collected and used as freshly prepared nanoparticle dispersions for subsequent studies. The gelatin solution was used as control in this work.

Scanning electron microscopy (SEM)

The freshly prepared BBG/Cur nanoparticle dispersions were freeze-dried, attached on the conductive adhesive, coated with a platinum layer, and examined by SU5000 scanning electron microscope (Hitachi, Tokyo, Japan) (Yang et al., 2022). The accelerating voltage was 5.0 kV. The magnification used were 100, 1000, and 20000×. The working distances were optimized to obtain clear characteristics in the images. The particle sizes in the SEM images were measured to calculate the average value ± standard deviation (n = 304).

Atomic force microscopy (AFM)

The freshly prepared nanoparticle dispersions were diluted (10 times) with ultrapure water and the pH was adjusted to 3.0, 5.0, 7.0, 9.0, or 11.0. Then, muscovite mica surfaces were freshly cleaved 10 μL of the samples were added. After left for 12 h, the samples were imaged by an AFM (Bioscope Resolve, Bruker Corp., Signal Hill, CA, USA) (Yang et al., 2022). The scan rate was 1.0 Hz. The operation mode was ScanAsyst in Air mode. The cantilever was SNL-series silicon cantilever (Bruker Corp.) with a spring constant of 0.35 N/m. The images were flattened and then the nanoparticle sizes were analyzed using the "Section" function in the commercial software.

Attenuated total reflectance-Fourier transform infrared (ATR-FTIR) spectrometry and secondary structure percentage analysis

The freshly prepared nanoparticle dispersions were freeze-dried and then examined by a Spotlight 400 ATR-FTIR spectrometer (PerkinElmer Company, USA) (Xu, Yang et al., 2022). The scanning number was 16. The wavenumber range was 4000–600 cm^{-1}. The scanning resolution was 4 cm^{-1}. The PeakFit v4.12 software (SeaSolve software Inc., Framingham, CA, USA) was used to analyze the secondary structure percentages of the nanoparticles by fitting the ATR-FTIR spectra at 1700–1600 cm^{-1}.

Zeta (ζ)-potential

Briefly, the freshly prepared nanoparticle dispersions were diluted (10 times) and the pH was adjusted to 3.0, 5.0, 7.0, 9.0, or 11.0. Then, the samples were examined using a Zeta-sizer Nano-ZS instrument (Malvern Instruments, Worcestershire, UK) at 25 °C (Li, et al., 2022). The fixed scattering angle was 175°. The Zeta potential values were calculated by the instrument commercial software with the Smoluchowski model.

Encapsulation efficiency (EE) and loading capacity (LC)

The absorbances of curcumin with different concentrations in ethanol aqueous solution (4:1, V/V) were determined by a Model T6 UV–visible spectrophotometer (Persee, Beijing, China) at 426 nm to build a standard curve (y = 0.1365x + 0.006; y range: 0.271–1.909; x range: 2–14 μg/mL; R^2 = 0.9997). The freshly prepared nanoparticle dispersion was diluted with ethanol solution (1:4, V/V). The mixture was ultrasonically treated for 10 min to extract curcumin into ethanol and was centrifuged at 1375 × g for 20 min to remove any precipitates. The obtained sample was diluted to an appropriate concentration (the absorbance should be in the absorbance range of standard curve) and the sample absorbance was measured at 426 nm. Finally, EE and LC of the gelatin nanoparticle were calculated by the following equations (Xiao, Nian & Huang, 2015; Dai, et al., 2018):

$$EE\,(\%) = \frac{Encapsulated\ curcumin\ (mg)}{Added\ curcumin\ (mg)} \times 100 \qquad (1)$$

$$LC\,(\%) = \frac{Encapsulated\ curcumin\ (mg)}{Added\ gelatin\ (mg)} \times 100 \qquad (2)$$

Emulsion preparation

The fish oil-loaded Pickering emulsions stabilized by curcumin-encapsulated particles were prepared (Zhang, Sun, Ding, Tao et al., 2020). Briefly, the pH of freshly prepared BBG/Cur nanoparticle dispersions was adjusted to 3.0, 5.0, 7.0, 9.0, and 11.0. Then, 5 mL of the dispersions were added to 5 mL of fish oil. The emulsions were prepared by mechanical homogenization of the mixtures (speed, 11500 rpm; time, 1 min) by a T10 homogenizer (10 mm head, IKA, Guangzhou City,

Guangdong Province, China). The emulsions were stored at room temperature (20–24 °C).

Emulsifying parameters of curcumin-encapsulated particle

Briefly, the emulsions were prepared as described in last section. Then, at 0 and 10 min, 20 μL of the emulsions were diluted (300 times) with sodium dodecyl sulfate solution (0.001 g/mL) and vortexed for 10 s. The sample absorbances were determined using a Model T6 UV–visible spectrophotometer at 500 nm. Finally, the emulsion activity index (EAI) and emulsion stability index (ESI) of curcumin-encapsulated particle were calculated as follows (Zhang et al., 2022):

$$\text{EAI} \, (\text{m}^2/\text{g}) = \frac{2 \times 2.303 \times A_0 \times N}{\varphi \times C \times 10000} \tag{3}$$

$$\text{ESI} \, (\text{min}) = \frac{A_0 \times \Delta t}{A_0 - A_{10}} \tag{4}$$

where A_0 and A_{10} are the measured absorbance at 0 min and 10 min, respectively, C is the protein weight per unit volume, N is the diluted factor, and φ is the oil volume fraction, and Δt is the time interval. EAI and ESI of pure BBG were determined as controls.

Droplet size analyses

Briefly, 3 μL of liquid emulsions or 3 mg of emulsion gel were examined by an optical microscope (ML 8000, Minz Precision, Shanghai, China) with a 40 × objective (Zhang, Sun, Ding, Tao et al., 2020). Three different batches were performed and then the images were randomly selected (3–5 images for each sample and at least one image for each batch). The sizes of all droplets (700–4100) in the selected images were analyzed by Image J software 1.53q (Wayne Rasband, National Institutes of Health, Bethesda, MD, USA) and frequency distribution with bin sizes of 2.5 μm or 1.0 μm. Finally, possible multimodal distribution was analyzed by Gauss fitting.

Emulsion appearance and creaming index

Briefly, the emulsions in glass vials were photographed. The creaming index (CI) values (%) were calculated by dividing the bottom serum layer heights by the whole emulsion heights and then multiplying by 100.

Lipid oxidation of the emulsions

Lipid hydroperoxide concentrations of the fish oil-loaded emulsions stabilized by BBG/Cur nanoparticles and BBG at different times were measured (Xu, Huang et al., 2022). Briefly, 1 mL of the emulsion was mixed with 7.5 mL of chloroform/methanol (2:1, v/v) by Vortexing for 2 min. It was centrifuged at 3000 × g for 5 min. Then, 1 mL of the mixture was diluted with methanol/1-butanol (2:1, v/v). The diluted solution was mixed with 15 μL of NH_4SCN (3.94 mol/L) and 15 μL of freshly-prepared ferrous iron solution (0.132 mol/L $BaCl_2$ and 0.144 mol/L $FeSO_4$). The mixture was Vortexed for 10 s and stood for 20 min in dark. Its absorbance was analyzed at 510 nm using a Model T6 UV–visible spectrophotometer. The lipid hydroperoxide concentration was determined by comparing with a standard curve of cumene hydroperoxide. The obtained values at different times were subtracted by the obtained values at 0 day.

Statistical analysis

The data were expressed as mean value ± standard deviation (n = 3). Statistical comparison in this work was performed by One-way ANOVA method (*p*-value < 0.05) in Statistical Package for the Social Sciences

(SPSS) 27 software (IBM Corp., Armonk, New York, USA).

Results

Preparation and characterization of BBG/Cur nanoparticle

Using a pH-cycle method, BBG/Cur nanoparticle was prepared. As shown in the SEM results, freeze-dried BBG/Cur nanoparticle sample consisted of sheet-like structures (Fig. 1A). Moreover, in the zoomed-in SEM images with larger magnification (Fig. 1B–C), some nanoparticles with a size of 343 ± 84 nm (Fig. S1) were attached on the sheet-like structures. In addition, some smaller nanoparticle-like structures were also present among these nanoparticles in Fig. 1C, which suggested that the nanoparticles with a size of 343 ± 84 nm were self-assembled from the smaller nanoparticle-like structures during the freeze-drying process. However, freeze-dried BBG sample (Fig. 1D–F) did not show obvious nanoparticles on the BBG sheet-like structures, which was consistent with our previous AFM results that BBG formed film-like nanostructures with a thickness of 2.8–3.2 nm on mica surface (Zhang, Sun, Ding, Li et al., 2020). In order to analyze the BBG/Cur nanoparticle size at single nanoparticle level, AFM was applied to determine the nanoparticle size after drying the samples at low concentration on mica surface. AFM results showed BBG/Cur sample consisted of nanoparticles at pH 3.0–11.0 (Fig. 1G–K). Moreover, the particle sizes at basic pH were lower than those at acidic and neutral pH (Fig. 1L). All the SEM and AFM results confirmed the successful preparation of BBG/Cur nanoparticle in this work. Moreover, the BBG/Cur nanoparticle showed similar sizes at acidic and neutral pH and decreased sizes at basic pH.

BBG/Cur nanoparticle, BBG, and curcumin were analyzed using ATR-FTIR spectrometry (Fig. 2A). BBG/Cur nanoparticle showed similar spectra shape to BBG. In addition, BBG/Cur nanoparticle also showed some characteristic peaks of curcumin (1513 cm^{-1}, 966 cm^{-1}, and 866 cm^{-1}, as indicated by dotted lines in Fig. 2A). Therefore, the obtained nanoparticle consisted of both BBG and curcumin. Further, PeakFit software analyzed the spectra of BBG/Cur nanoparticle and BBG at 1700–1600 cm^{-1} by a deconvolution method (Fig. S2). The peak areas with the peak values at 1610–1642 cm^{-1} (β-sheet), 1642–1650 cm^{-1} (random coil), 1650–1660 cm^{-1} (α-helix), 1660–1680 cm^{-1} (β-turn), and 1680–1700 cm^{-1} (β-antiparallel) were analyzed to calculate the secondary structure percentages. As shown in Fig. 2B, BBG/Cur nanoparticles showed similar secondary structure percentages to BBG: β-sheet > β-turn ≈ random coil ≈ α-helix > β-antiparallel, which accorded with pepsin enzyme-extracted tilapia skin gelatin and silver carp scale gelatin) (Xu, et al., 2021; Zhang, et al., 2022). Therefore, the formation of BBG/Cur nanoparticles did not obviously change the secondary structure percentages of BBG.

The Zeta potential of the BBG/Cur nanoparticle dispersions was measured (Fig. 2C). The Zeta potential values decreased with the increasing solution pH, which accorded with the trend of gelatin nanoparticle (Tan, Zhang, Han, Zhang & Ngai, 2022). Moreover, BBG/Cur nanoparticle dispersions (Fig. 2C) showed zero Zeta potential at pH 3.0–5.0. Considering that BBG showed an isoelectric point of 5.0 according to the turbidity experiment (Zhang, Sun, Ding, Li et al., 2020), the formation of BBG/Cur particles might decrease the isoelectric point to 3.0–5.0. They further confirmed that the isoelectric point of BBG was 5.0 and the presence of curcumin in the nanoparticle slightly changed the Zeta potential.

The EE and LC of curcumin in the BBG/Cur nanoparticle were measured (Xiao, et al., 2015; Dai, et al., 2018). The EE and LC of curcumin were 93.9 ± 0.5 % and 9.4 ± 0.1 %, respectively. The EE value (93.9 ± 0.5 %) suggested that the nanoparticle could efficiently encapsulate curcumin. The LC value (9.4 ± 0.1 %) suggested BBG was the matrix material and curcumin was the encapsulated material. Therefore, pH-cycle method was an efficient method to prepare hydrophilic gelatin nanoparticle for encapsulating curcumin.
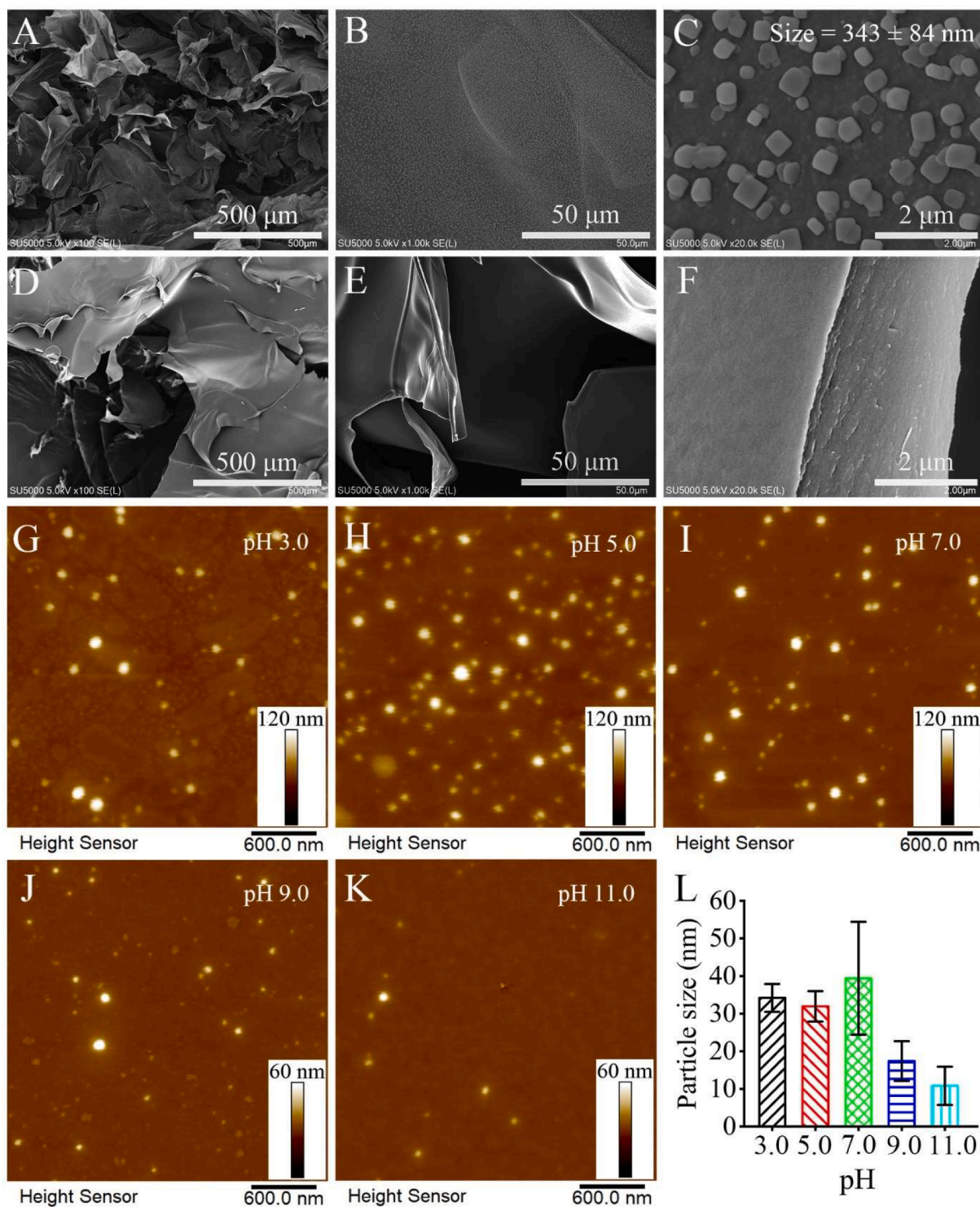
Fig. 1. Morphologies of curcumin-encapsulated bovine bone gelatin (BBG/Cur) nanoparticles. (A–C): Scanning electron microscopy images of BBG/Cur nanoparticles with different magnification. (D–F): Scanning electron microscopy images of BBG with different magnification. (G–K): Atomic force microscopy height images of BBG/Cur at different pH. (L): The particle sizes of BBG/Cur nanoparticles in atomic force microscopy height images.

Preparation and characterization of fish oil-loaded emulsions stabilized by BBG/Cur nanoparticle at different pH

The fish oil-loaded emulsions stabilized by BBG/Cur nanoparticle and BBG at different pH were prepared. As shown in Fig. 3A–B, the BBG/Cur nanoparticle-stabilized emulsions were in yellow (pH 3.0–9.0) and orange (pH 11.0), which were different to the white color of BBG-stabilized emulsions. Therefore, the yellow and orange colors were

attributed to the presence of curcumin. The freshly-prepared emulsions comprised of microscale droplets (Fig. 3C) with trimodal distribution (Fig. 3D–E). It also should be noted that some extra-large droplets were present in the emulsions (Fig. 3C) that were not fitted in the trimodal distribution due to their low frequency (Figs. S4–S5). It is obvious that the emulsions stabilized by BBG/Cur nanoparticles showed similar droplet sizes to that stabilized by BBG. Moreover, the droplet sizes were dependent on solution pH: pH 3.0 > pH 5.0 ≈ pH 7.0 ≈ pH 9.0 > pH
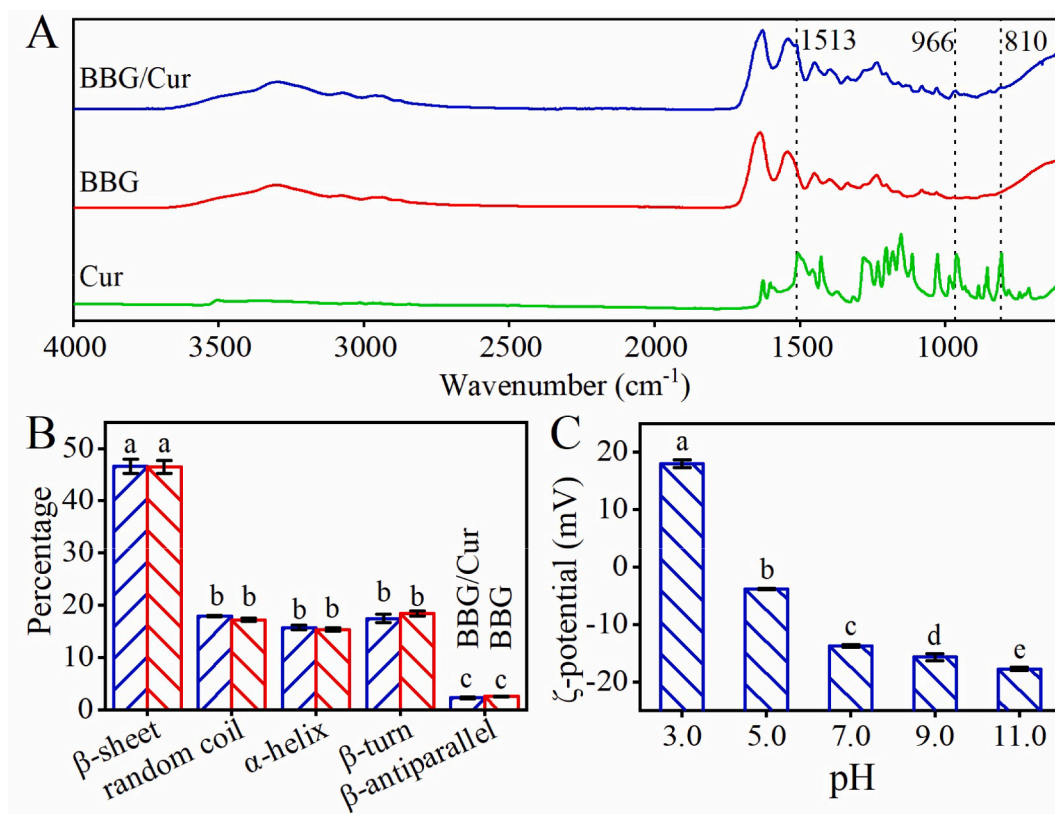
Fig. 2. ATR-FTIR spectra (A), secondary structure percentages (B), and Zeta potential (C) of BBG/Cur nanoparticles. BBG and curcumin were used as controls. For the columns in each image, different letters indicate significant differences ($p < 0.05$).

11.0.

Emulsifying parameters of BBG/Cur nanoparticle

Emulsifying parameters (EAI and ESI) of the emulsions stabilized with BBG/Cur nanoparticle and BBG were analyzed by using fish oil-loaded emulsion (water/oil ratio of 1:1 and pH 7.0) as the model system. The EAI and ESI for emulsions stabilized with BBG were 19.7 ± 0.4 m^2/g and 360.3 ± 30.5 min, respectively. These data were comparable to the data (EAI of 30.9 ± 0.6 m^2/g and ESI of 267.8 ± 2.1 min) for the fish oil-loaded emulsions (water/oil ratio of 2:1 and pH 9.0) stabilized by BBG at the same concentration (Zhang, Sun, Ding, Li et al., 2020). The EAI and ESI of the emulsions stabilized by BBG/Cur nanoparticles were 25.1 ± 0.9 m^2/g and 161.5 ± 18.8 min, respectively. Emulsions stabilized with BBG/Cur nanoparticle showed higher EAI and lower ESI than the one stabilized with BBG. Therefore, the nanoparticle formation increased the emulsifying activity ability and decreased the emulsifying stability ability of BBG.

Emulsion storage stability at different pH

During the storage at room temperature, the emulsions stabilized with BBG/Cur nanoparticles at different pH were observed by a digital camera (Fig. 4A–D) and an optical microscope (Fig. 4E). The liquid-gel transition time depended on solution pH: pH 11.0 (more than 14 days) > pH 9.0 (7 days) > pH 3.0 (3 days) > pH 5.0 (one day) ≈ pH 7.0 (one day). All the emulsions did not show obviously droplet size increase even at day 14, which suggested BBG/Cur nanoparticles could inhibit droplet coalescence during the storage. Previous work suggested the emulsions stabilized with high concentrations (10–40 mg/mL) of BBG or crosslinked BBG nanoparticles could inhibit droplet coalescence (Ding, et al., 2020b). The used BBG concentration was 10 mg/mL for the BBG/Cur nanoparticle preparation in this work. Therefore, the droplet

stability might be mainly dependent on the nanoparticle concentration. Finally, the emulsions at day 14 showed different creaming index values during the storage (Fig. 4F): pH 11.0 (0 %, n = 3, the same as below) < pH 7.0 (4.4 ± 1.8 %) ≈ pH 5.0 (4.5 ± 1.7 %) ≈ pH 9.0 (6.1 ± 2.0 %) < pH 3.0 (24.8 ± 1.4 %).

Lipid oxidation of the emulsions

The lipid hydroperoxide values of fish oil-loaded emulsions stabilized by BBG/Cur nanoparticles and BBG at different pH were analyzed at different time points during the storage at room temperature (Fig. 5). Compared with pure fish oil, the encapsulation of fish oil by BBG- or BBG/Cur nanoparticle-stabilized emulsions could retard the lipid oxidation (Fig. 5), which was consistent with the encapsulation of fish oil by silver carp scale gelatin-stabilized emulsions (Xu, Huang et al., 2022). The emulsions stabilized by BBG nanoparticles showed lower lipid hydroperoxides than the emulsions stabilized by BBG at all the pH. It suggested that the presence of curcumin in BBG/Cur nanoparticles could provide a certain antioxidant effect (Fig. 5), which was consistent with the presence of curcumin in soybean protein isolate/Cur nanoparticles (Du et al., 2022). Moreover, the lipid hydroperoxide values of the emulsions stabilized by both BBG/Cur nanoparticles and BBG were dependent on pH: pH 11.0 < pH 9.0 < pH 7.0 ≈ pH 5.0 < pH 3.0 < fish oil.

Discussion

Formation and properties of BBG/Cur nanoparticle

As shown in Fig. 6A, curcumin has three hydroxy groups in the molecular structure. The isoelectric point of BBG is pH 5.0 (Zhang, Sun, Ding, Li et al., 2020). Therefore, pH-cycle method was explored to prepare BBG/Cur nanoparticle in this work (Fig. 6B). At pH 12.0, the
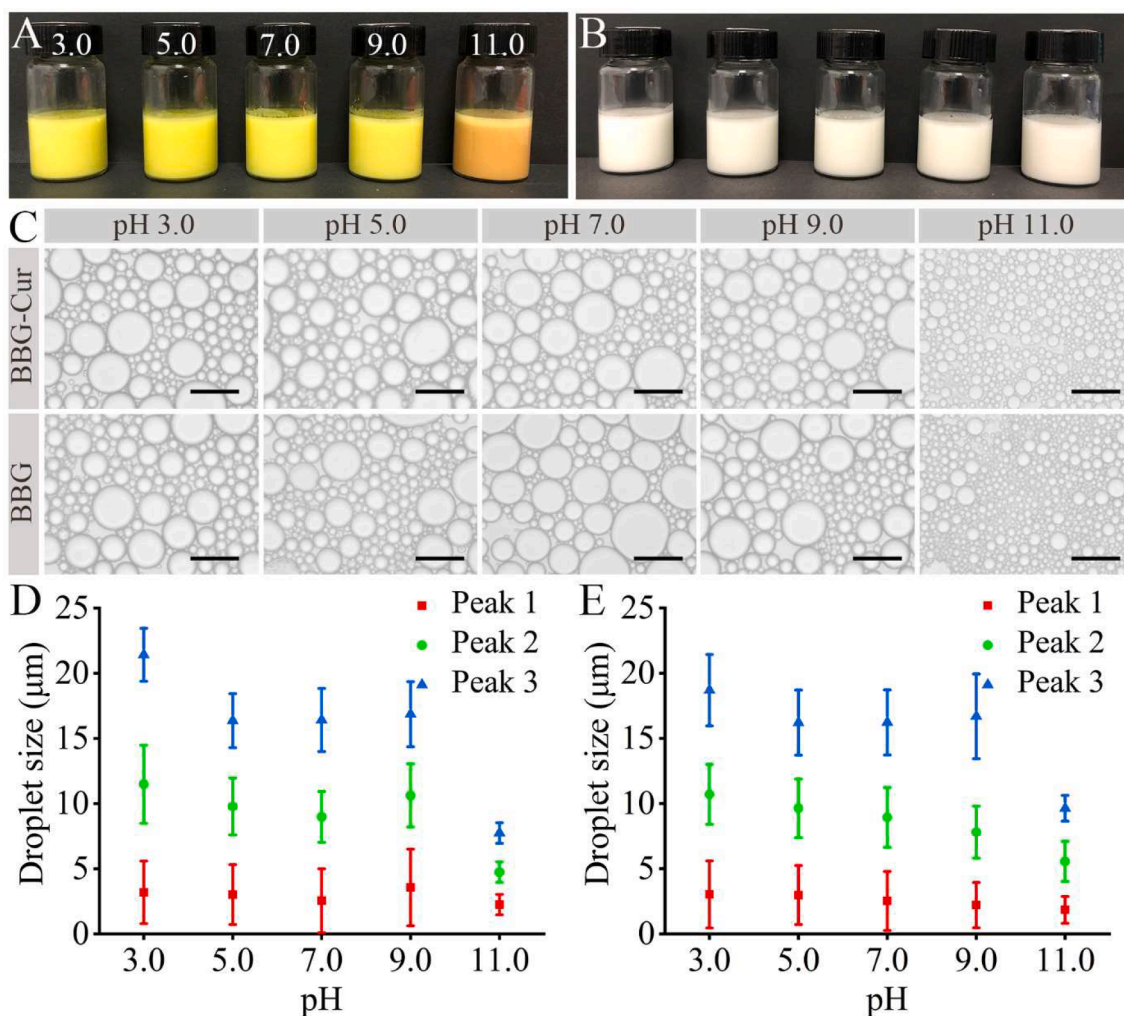
Fig. 3. Newly-prepared fish oil-loaded emulsions stabilized by BBG/Cur nanoparticles (A and D) and BBG (B and E) at different pH. (A–B): Digital camera images. (C): Optical microscopy images. Black scale bars indicate 40 μm. (D–E): The most probable sizes of the emulsion droplets.

deprotonation induced the formation of the negative charges of BBG and curcumin, which led to the dissociation of BBG and the dissolution of curcumin. Therefore, BBG and curcumin were well blended at the strong alkaline environment (Zhan et al., 2020). When the solution pH was back to 7.0, the molecular re-protonation decreased their solubility and the intramolecular charge repulsion, enabling the refolding of BBG and the interaction of BBG with curcumin to produce BBG/Cur nanoparticle.

SEM (Fig. 1A–F) and AFM (Fig. 1G–L) results confirmed the successful preparation of BBG/Cur nanoparticle. Moreover, the particle sizes depended on solution pH (Fig. 1L): pH 7.0 > pH 3.0 > pH 5.0 > pH 9.0 > pH 11.0. ATR-FTIR spectrometry (Fig. 1A) confirmed the co-existence of BBG and curcumin in the nanoparticle. Further, the ATR-FTIR spectrometry-based secondary structure percentage analyses (Fig. 1B) showed nanoparticle formation had no obvious effect on BBG secondary structure percentages, which implied that the interaction of BBG with curcumin did not obviously affect the refolding of BBG. Zeta potential results (Fig. 2C) showed Zeta potential decreased with the increase of the solution pH, which suggested functional groups of BBG and curcumin in the nanoparticle could be deprotonated or re-protonated by adjusting the solution pH.

The EE and LC of curcumin in the BBG nanoparticle were 93.9 ± 0.5 % and 9.4 ± 0.1 %, respectively. They were higher than those of kafirin/curcumin nanoparticles (EE, 55.0 ± 1.1 %; LC, 5.0 ± 0.1 %) and kafirin/carboxymethyl chitosan/curcumin nanoparticles (EE, 86.1 ± 2.1 %; LC, 6.1 ± 0.2 %) (Xiao et al., 2015). The EE of curcumin in BBG/Cur

nanoparticle was also higher than those of zein/curcumin nanoparticle (17.20 %) and similar to those of zein/rhamnolipid/curcumin nano-particles (89.50 ± 0.500 %–98.78 ± 0.225 %) (Dai et al., 2018). Especially, the LC of curcumin in BBG/Cur nanoparticle was higher than those (<3.24 ± 0.01 %) of zein/curcumin nanoparticle and zein/rhamnolipid/curcumin nanoparticle (Dai et al., 2018). Therefore, hydrophilic gelatin is an excellent matrix material to prepare curcumin-encapsulated protein nanoparticles with extra higher EE and LC than many proteins.

Effect of BBG/Cur nanoparticle on the formation and stability of fish oil-loaded emulsions at different pH

BBG/Cur nanoparticle was applied to stabilize fish oil-loaded Pickering emulsions at different solution pH (Figs. 3–5 and 6C). The obtained Pickering emulsions showed yellow (pH 3.0–9.0) and orange (pH 11.0) colors due to the presence of curcumin (Fig. 3A–B). As shown in Fig. 3C–E, the emulsions stabilized by BBG/Cur nanoparticle and BBG consisted with microscale droplets with trimodal distribution. Therefore, nanoparticle formation by the pH-cycle method did not affect the multiple peak distribution of emulsion droplets, which was consisted with the nanoparticle formation by chemically crosslinking method (Ding et al., 2019, 2020b).

The droplet sizes of the Pickering emulsions were dependent on solution pH: pH 3.0 > pH 5.0 ≈ pH 7.0 ≈ pH 9.0 > pH 11.0 (Fig. 3D–E).
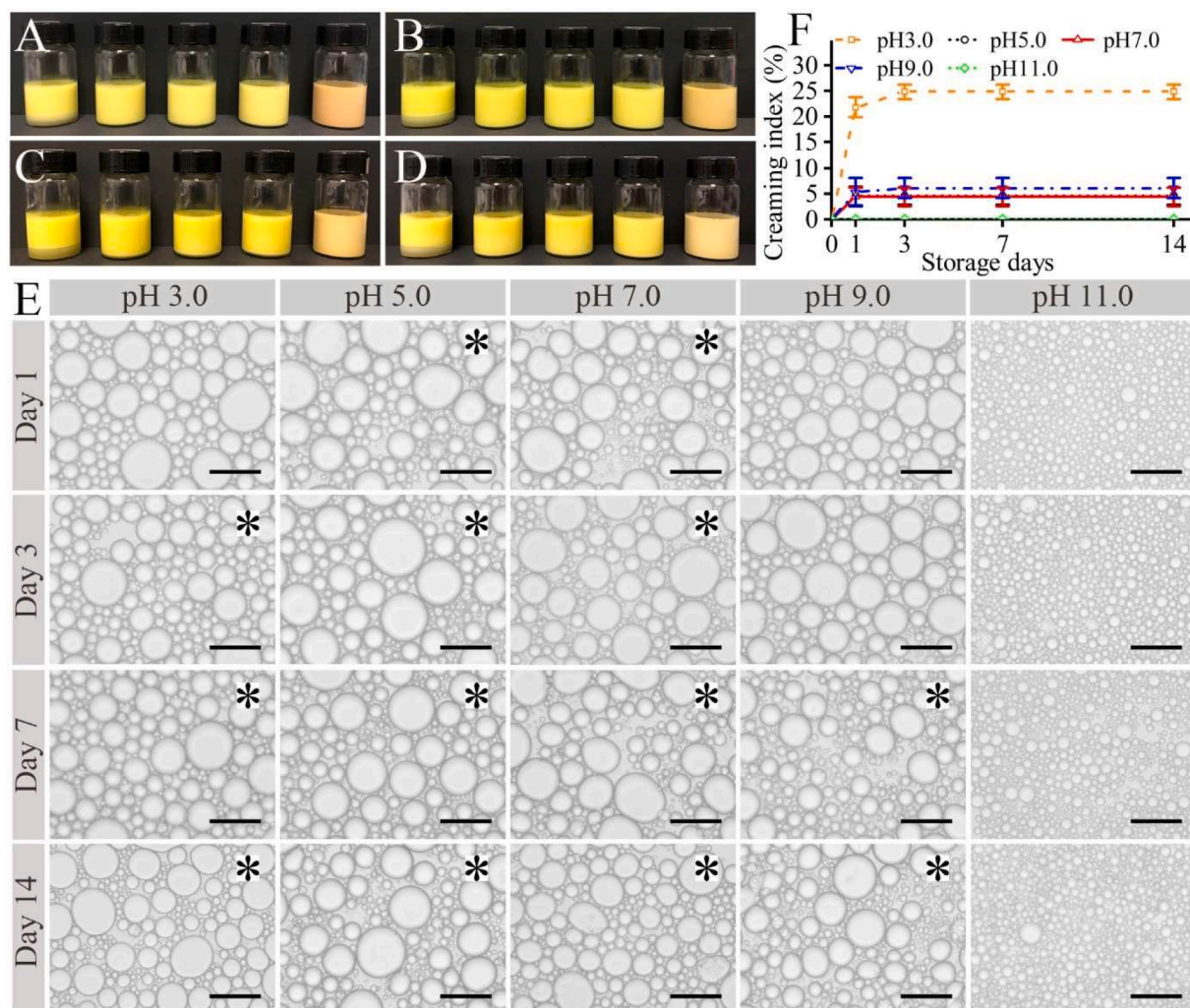
Fig. 4. Stability of fish oil-loaded emulsions stabilized by BBG/Cur nanoparticles at different pH during the storage at room temperature. (A–D): Digital camera images at day 1, 3, 7, and 14, respectively. (E): Optical microscopy images. Black scale bars indicate 40 μm. Black asterisks indicate emulsion gels and others are liquid emulsions. (F): Creaming index values of fish oil-loaded emulsions stabilized by BBG/Cur nanoparticles.

Previous paper demonstrated that the Pickering emulsion droplet sizes usually decreased with the decrease of nanoparticle sizes (Matos, Marefati, Bordes, Gutiérrez & Rayner, 2017). The order of the Zeta potential (Fig. 2C) was: pH 3.0 > pH 5.0 > pH 7.0 > pH 9.0 > pH 11.0. The order of absolute charges (absolute Zeta potential) of BBG/Cur nanoparticles was: pH 3.0 ≈ pH 11.0 > pH 9.0 > pH 7.0 > pH 5.0 (Fig. 2C). The size order of BBG/Cur nanoparticle at different pH was (Fig. 1L): pH 7.0 > pH 3.0 > pH 5.0 > pH 9.0 > pH 11.0. Although the sample at pH 7 shows a larger mean value for the particle size, the standard deviation between the measurements was higher than others. Some values at pH 7.0 were smaller than what was measured at pH 5. It could be clearly observed that for larger particle at low pH value of 3, the Zeta potential value was positive. Moreover, as the pH increased, the Zeta potential value became more negative and the smaller particles produced at higher pH should showed better emulsifying properties due to the presence of electrostatic repulsion and resistance to aggregation as was evidenced by Fig. 3C at pH 11, where smaller emulsion droplets were produced due to contribution of smaller-sized particles with a higher negative charge to a higher emulsion stability. Our work was consistent with a previous work, which suggested the emulsion droplet size increased and the absolute Zeta potential decreased with the increase of pH (Cai, Wang, Du, Xing & Zhu, 2020). Moreover, no obvious droplet size increase was observed during the storage (Fig. 4), which suggested BBG/Cur nanoparticles could inhibit droplet coalescence. It was significantly different

to the obvious droplet coalescence of BBG-stabilized traditional emulsions (Ding et al., 2021).

EAI and ESI are quantitative data to analyze the emulsifying properties of an emulsifier. According to the results in Section 3.3, BBG/Cur nanoparticle (25.1 ± 0.9 m^2/g) had higher EAI value than BBG (19.7 ± 0.4 m^2/g), whereas BBG/Cur nanoparticle (161.5 ± 18.8 min) had lower ESI value than BBG (360.3 ± 30.5 min). Previous work suggested that gelatins are relatively weaker emulsifiers (Zhang, Xu et al., 2020). The size (greater than 10 nm) of BBG/Cur nanoparticles (Fig. 1L) was generally larger than the thickness (2.8–3.2 nm) of film-like nanostructures for BBG (Zhang, Sun, Ding, Li et al., 2020). BBG/Cur nanoparticle might increase the emulsion interfacial layer thickness compared with BBG (nanoparticle layer thickness > BBG molecule layer thickness) and therefore increase EAI (area of oil/water interface stabilized by per unit weight of protein), whereas BBG/Cur nanoparticle might decrease the compactness and increase the gap between nanoparticles at the oil/water interface (Fig. 6C), which decreased ESI (time needed to achieve a turbidity of the emulsion that is one-half of its original value) (Chatterjee, Dey, Ghosh & Dhar, 2015). In order to increase ESI values in the future, the gap among the nanoparticles at the emulsion interfaces should be decreased. Considering that higher emulsifier concentration could induce high ESI value (Ashaolu & Zhao, 2020), a simple way was to increase BBG/Cur nanoparticle concentration. Another way was to decrease the nanoparticle size in the pH-cycle
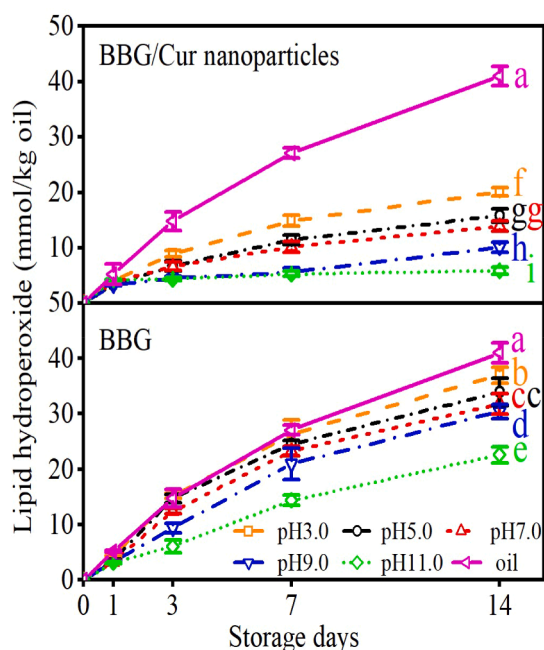
Fig. 5. Lipid hydroperoxide values of of fish oil-loaded emulsions stabilized by BBG/Cur nanoparticles and BBG at different pH during the storage at room temperature. For the values at day 14, different letters indicate significant differences ($p < 0.05$).

method, and therefore, more nanoparticles could be present at the emulsion interface to decrease the gaps.

According to the physical state, emulsions can be classified into liquid emulsions and emulsion gels (both gel and droplets are present in the soft-solid colloid material). Gelatin-based emulsion gels are generally produced because of the self-assembled helices formation of gelatin during the storage at the temperature below 30 °C (Gómez-Guillén, Giménez, López-Caballero & Montero, 2011; Lin, Kelly & Miao, 2020). In this work, the obtained BBG/Cur nanoparticle-stabilized Pickering emulsions showed different liquid-gel transition times at different

solution pH (Fig. 4): pH 11.0 (more than 14 days) > pH 9.0 (7 days) > pH 3.0 (3 days) > pH 5.0 (one day) ≈ pH 7.0 (one day). Therefore, the formation of gelatin self-assembled helices structures was dependent on solution pH. Our previous papers showed, during the storage, fish oil-loaded emulsions stabilized by BBG, cold-water fish skin gelatin, and silver carp scale gelatin showed liquid-gel transition (Zhang, Sun, Ding, Li et al., 2020; Xu et al., 2021). Moreover, the liquid-gel transition time was increased by gelatin nanoparticle preparation (Ding et al., 2020b), pH adjustment (Ding et al., 2020a), and acylation modification (Zhang et al., 2022). This work further suggested the liquid-gel transition time of Pickering emulsions was also dependent on solution pH.

During the storage (Fig. 4), the Pickering emulsions at pH equal to 3.0 showed obvious creaming, the Pickering emulsions at pH equal to 5.0–9.0 showed slight creaming, whereas the Pickering emulsions at pH equal to 11.0 showed no obvious creaming. The emulsion droplet move speed (V_{stokes}) can be described by Stokes' Law (McClements & Jafari, 2018):

$$V_{stokes} = -\frac{2gr^2(\rho_2 - \rho_1)}{9\eta_1} \tag{5}$$

where g is gravity acceleration, r is the initial droplet radius, ρ_2 is the dispersed phase density, ρ_1 is the water phase density, and η_1 is the water phase shear viscosity.

In this work, the initial droplet radius (r) might be the main factor for creaming stability. The initial droplet size ($2r$) order was (Fig. 3D): pH 11.0 < pH 5.0 ≈ pH 7.0 ≈ pH 9.0 < pH 3.0. According to the Eq. (5), the V_{stokes} order was the same to the droplet size order. Therefore, the creaming index order was also the same to the droplet size order (Fig. 4). It also suggested that small initial droplet sizes were required for ideal creaming stability of BBG/Cur nanoparticle-stabilized emulsions. Considering that the droplet sizes of Pickering emulsions usually decreased with the decrease of nanoparticle size (Matos et al., 2017), smaller BBG/Cur nanoparticles might be required for emulsions.

The emulsion creaming stability is an important purpose for the emulsion research. The Pickering emulsion creaming stability increased with the decrease of the initial droplet size according to Stokes' Law (Eq. (5)). As discussed above in this section, the initial droplet sizes were at least affected by the nanoparticle size and nanoparticle surface charge. The initial droplet sizes of Pickering emulsions usually decreased with
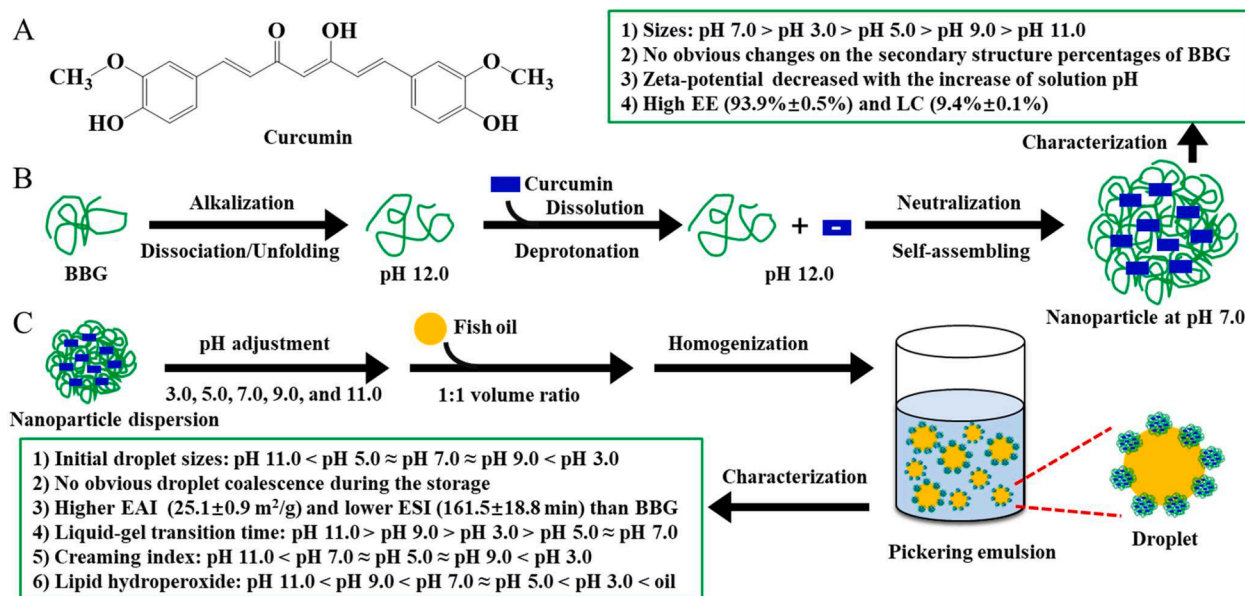

Fig. 6. Schematics of BBG/Cur nanoparticle for emulsion development. (A): Molecular structure of curcumin. (B): Preparation and characterization of BBG/Cur nanoparticle by a pH-cycle method. The particle had high encapsulation efficiency (EE) and loading capacity (LC). (C): Application of BBG/Cur nanoparticle for the stabilization of fish oil-loaded emulsion. See main text for details.

the decrease of nanoparticle sizes (Matos et al., 2017) and the increase of the absolute Zeta potential (Cai et al., 2020). Therefore, in order to prepare more stable Pickering emulsions, further studies are required to explore the preparation of BBG/Cur nanoparticles with lower sizes and higher surface charges. For example, the lower BBG concentration in the nanoparticle preparation process might be considered to prepare nanoparticle with lower size. The application of modified BBG with more charges might be also considered to prepare nanoparticle with higher surface charge.

Finally, lipid hydroperoxide values of fish oil-loaded emulsions were also analyzed (Fig. 5). Curcumin in BBG/Cur nanoparticles could provide a certain antioxidant effect (Fig. 5). Moreover, pH had obvious effect on the lipid hydroperoxide values of the emulsions stabilized by both BBG/Cur nanoparticles and BBG (Fig. 6): pH 11.0 < pH 9.0 < pH 7.0 ≈ pH 5.0 < pH 3.0 < fish oil. Further work is required to analyze the underlying effect mechanism of pH on the lipid oxidation of fish oil-loaded emulsions stabilized by BBG/Cur nanoparticles.

Conclusions

In this work, curcumin-encapsulated hydrophilic gelatin nanoparticle was prepared by a pH-cycle method and applied for fish oil-loaded emulsions. The obtained results confirmed pH-cycle method could be applied to prepare hydrophilic gelatin nanoparticle. Moreover, the obtained curcumin-encapsulated hydrophilic gelatin nanoparticle could be applied to stabilize oil-in-water Pickering emulsions. This work enlarged the potential application range of pH-cycle method in the field of protein science, nanoparticle science, and emulsion science. It also provided a promising idea of nutrient-encapsulated emulsifiers, and therefore, hydrophobic nutrients could be present in the oil/water interface (not necessary in the oil phase in the traditional method). Finally, this work provided important information for the development and application of hydrophobic antioxidant-encapsulated hydrophilic protein nanoparticle to stabilize oil-in-water Pickering emulsions.

CRediT authorship contribution statement

Guangyi Kan: Investigation, Data curation, Writing – original draft. **Ye Zi:** Investigation. **Li Li:** Investigation. **Huan Gong:** Investigation. **Jiawei Peng:** Investigation. **Xichang Wang:** Resources. **Jian Zhong:** Conceptualization, Supervision, Data curation, Writing – review & editing.

Declaration of Competing Interest

The authors declare that they have no known competing financial interests or personal relationships that could have appeared to influence the work reported in this paper.

Data availability

Data will be made available on request.

Appendix A. Supplementary data

Supplementary data to this article can be found online at https://doi.org/10.1016/j.fochx.2023.100590.

References:

Alipal, J., Mohd Pu`ad, N. A. S., Lee, T. C., Nayan, N. H. M., Sahari, N., Basri, H., … Abdullah, H. Z. (2021). A review of gelatin: Properties, sources, process, applications, and commercialisation. *Materials Today: Proceedings, 42*, 240–250. https://doi.org/10.1016/j.matpr.2020.12.922

Ashaolu, T. J., & Zhao, G. (2020). Fabricating a Pickering stabilizer from okara dietary fibre particulates by conjugating with soy protein isolate via maillard reaction. *Foods, 9*, 143. https://doi.org/10.3390/foods9020143

Cai, X., Wang, Y., Du, X., Xing, X., & Zhu, G. (2020). Stability of pH-responsive Pickering emulsion stabilized by carboxymethyl starch/xanthan gum combinations. *Food Hydrocolloids, 109*, Article 106093. https://doi.org/10.1016/j.foodhyd.2020.106093

Cao, H., Yang, L., Tian, R., Wu, H., Gu, Z., & Li, Y. (2022). Versatile polyphenolic platforms in regulating cell biology. *Chemical Society Reviews, 51*, 4175–4198. https://doi.org/10.1039/D1CS01165K

Chatterjee, R., Dey, T. K., Ghosh, M., & Dhar, P. (2015). Enzymatic modification of sesame seed protein, sourced from waste resource for nutraceutical application. *Food and Bioproducts Processing, 94*, 70–81. https://doi.org/10.1016/j.fbp.2015.01.007

Dai, L., Li, R., Wei, Y., Sun, C., Mao, L., & Gao, Y. (2018). Fabrication of zein and rhamnolipid complex nanoparticles to enhance the stability and in vitro release of curcumin. *Food Hydrocolloids, 77*, 617–628. https://doi.org/10.1016/j.foodhyd.2017.11.003

Ding, M., Liu, L., Zhang, T., Tao, N., Wang, X., & Zhong, J. (2021). Effect of interfacial layer number on the storage stability and in vitro digestion of fish oil-loaded multilayer emulsions consisting of gelatin particle and polysaccharides. *Food Chemistry, 336*, Article 127686. https://doi.org/10.1016/j.foodchem.2020.127686

Ding, M., Zhang, T., Zhang, H., Tao, N., Wang, X., & Zhong, J. (2019). Effect of preparation factors and storage temperature on fish oil-loaded crosslinked gelatin nanoparticle pickering emulsions in liquid forms. *Food Hydrocolloids, 95*, 326–335. https://doi.org/10.1016/j.foodhyd.2019.04.052

Ding, M., Zhang, T., Zhang, H., Tao, N., Wang, X., & Zhong, J. (2020a). Gelatin-stabilized traditional emulsions: Emulsion forms, droplets, and storage stability. *Food Science and Human Wellness, 9*, 320–327. https://doi.org/10.1016/j.fshw.2020.04.007

Ding, M., Zhang, T., Zhang, H., Tao, N., Wang, X., & Zhong, J. (2020b). Gelatin molecular structures affect behaviors of fish oil-loaded traditional and Pickering emulsions. *Food Chemistry, 309*, Article 125642. https://doi.org/10.1016/j.foodchem.2019.125642

Du, C.-X., Xu, J.-J., Luo, S.-Z., Li, X.-J., Mu, D.-D., Jiang, S.-T., & Zheng, Z. (2022). Low-oil-phase emulsion gel with antioxidant properties prepared by soybean protein isolate and curcumin composite nanoparticles. *LWT, 161*, Article 113346. https://doi.org/10.1016/j.lwt.2022.113346

Duconseille, A., Astruc, T., Quintana, N., Meersman, F., & Sante-Lhoutellier, V. (2015). Gelatin structure and composition linked to hard capsule dissolution: A review. *Food Hydrocolloids, 43*, 360–376. https://doi.org/10.1016/j.foodhyd.2014.06.006

Fu, X., Belwal, T., He, Y., Xu, Y., Li, L., & Luo, Z. (2020). Interaction and binding mechanism of cyanidin-3-O-glucoside to ovalbumin in varying pH conditions: A spectroscopic and molecular docking study. *Food Chemistry, 320*, Article 126616. https://doi.org/10.1016/j.foodchem.2020.126616

Gómez-Guillén, M. C., Giménez, B., López-Caballero, M. E., & Montero, M. P. (2011). Functional and bioactive properties of collagen and gelatin from alternative sources: A review. *Food Hydrocolloids, 25*, 1813–1827. https://doi.org/10.1016/j.foodhyd.2011.02.007

Huang, H., Belwal, T., Aalim, H., Li, L., Lin, X., Liu, S., … Luo, Z. (2019). Protein-polysaccharide complex coated W/O/W emulsion as secondary microcapsule for hydrophilic arbutin and hydrophobic coumaric acid. *Food Chemistry, 300*, Article 125171. https://doi.org/10.1016/j.foodchem.2019.125171

Jiang, J., Wang, Q., & Xiong, Y. L. (2018). A pH shift approach to the improvement of interfacial properties of plant seed proteins. *Current Opinion in Food Science, 19*, 50–56. https://doi.org/10.1016/j.cofs.2018.01.002

Karim, A. A., & Bhat, R. (2009). Fish gelatin: Properties, challenges, and prospects as an alternative to mammalian gelatins. *Food Hydrocolloids, 23*, 563–576. https://doi.org/10.1016/j.foodhyd.2008.07.002

Lei, L., Chen, Y.-L., Zhu, C.-H., Wu, H.-F., Wan, Z.-L., Yang, X.-Q., & Yuan, Y. (2022). The novel pickering emulsion gels stabilized by zein hydrolysate-chitin nanocrystals coacervates: Improvement on stability and bioaccessibility for curcumin. *Food Research International, 161*, Article 111877. https://doi.org/10.1016/j.foodres.2022.111877

Li, H., Zhang, X., Zhao, C., Zhang, H., Chi, Y., Wang, L., … Zhang, X. (2022). Entrapment of curcumin in soy protein isolate using the pH-driven method: Nanoencapsulation and formation mechanism. *LWT, 153*, Article 112480. https://doi.org/10.1016/j.lwt.2021.112480

Lin, D., Kelly, A. L., & Miao, S. (2020). Preparation, structure-property relationships and applications of different emulsion gels: Bulk emulsion gels, emulsion gel particles, and fluid emulsion gels. *Trends in Food Science & Technology, 102*, 123–137. https://doi.org/10.1016/j.tifs.2020.05.024

Matos, M., Marefati, A., Bordes, R., Gutiérrez, G., & Rayner, M. (2017). Combined emulsifying capacity of polysaccharide particles of different size and shape. *Carbohydrate Polymers, 169*, 127–138. https://doi.org/10.1016/j.carbpol.2017.04.006

McClements, D. J., & Jafari, S. M. (2018). Improving emulsion formation, stability and performance using mixed emulsifiers: A review. *Advances in Colloid and Interface Science, 251*, 55–79. https://doi.org/10.1016/j.cis.2017.12.001

Saffarionpour, S., & Diosady, L. L. (2022). Curcumin, a potent therapeutic nutraceutical and its enhanced delivery and bioaccessibility by pickering emulsions. *Drug Delivery*

and Translational Research, 12, 124–157. https://doi.org/10.1007/s13346-021-00936-3

Shah, B. R., Zhang, C., Li, Y., & Li, B. (2016). Bioaccessibility and antioxidant activity of curcumin after encapsulated by nano and Pickering emulsion based on chitosan-tripolyphosphate nanoparticles. *Food Research International, 89*, 399–407. https://doi.org/10.1016/j.foodres.2016.08.022

Sun, C., Gao, Y., & Zhong, Q. (2018). Effects of acidification by glucono-delta-lactone or hydrochloric acid on structures of zein-caseinate nanocomplexes self-assembled during a pH cycle. *Food Hydrocolloids, 82*, 173–185. https://doi.org/10.1016/j.foodhyd.2018.04.007

Tan, H., Zhang, R., Han, L., Zhang, T., & Ngai, T. (2022). Pickering emulsions stabilized by aminated gelatin nanoparticles: Are gelatin nanoparticles acting as genuine Pickering stabilizers or structuring agents? *Food Hydrocolloids, 123*, Article 107151. https://doi.org/10.1016/j.foodhyd.2021.107151

Wang, X.-Y., & Heuzey, M.-C. (2016). Pickering emulsion gels based on insoluble chitosan/gelatin electrostatic complexes. *RSC Advances, 6*, 89776–89784. https://doi.org/10.1039/C6RA10378B

Wu, T., Ding, M., Shi, C., Qiao, Y., Wang, P., Qiao, R., … Zhong, J. (2020). Resorbable polymer electrospun nanofibers: History, shapes and application for tissue engineering. *Chinese Chemical Letters, 31*, 617–625. https://doi.org/10.1016/j.cclet.2019.07.033

Xiao, J., Nian, S., & Huang, Q. (2015). Assembly of kafirin/carboxymethyl chitosan nanoparticles to enhance the cellular uptake of curcumin. *Food Hydrocolloids, 51*, 166–175. https://doi.org/10.1016/j.foodhyd.2015.05.012

Xu, J., Huang, S., Zhang, Y., Zheng, Y., Shi, W., Wang, X., & Zhong, J. (2022). Effects of antioxidant types on the stabilization and in vitro digestion behaviors of silver carp scale gelatin-stabilized fish oil-loaded emulsions. *Colloids and Surfaces B: Biointerfaces, 217*, Article 112624. https://doi.org/10.1016/j.colsurfb.2022.112624

Xu, J., Yang, L., Nie, Y., Yang, M., Wu, W., Wang, Z., … Zhong, J. (2022). Effect of transglutaminase crosslinking on the structural, physicochemical, functional, and emulsion stabilization properties of three types of gelatins. *LWT, 163*, Article 113543. https://doi.org/10.1016/j.lwt.2022.113543

Xu, J., Zhang, T., Zhang, Y., Yang, L., Nie, Y., Tao, N., … Zhong, J. (2021). Silver carp scale gelatins for the stabilization of fish oil-loaded emulsions. *International Journal of Biological Macromolecules, 186*, 145–154. https://doi.org/10.1016/j.ijbiomac.2021.07.043

Yang, L., Yang, M., Xu, J., Nie, Y., Wu, W., Zhang, T., … Zhong, J. (2022). Structural and emulsion stabilization comparison of four gelatins from two freshwater and two marine fish skins. *Food Chemistry, 371*, Article 131129. https://doi.org/10.1016/j.foodchem.2021.131129

Zhan, X., Dai, L., Zhang, L., & Gao, Y. (2020). Entrapment of curcumin in whey protein isolate and zein composite nanoparticles using pH-driven method. *Food Hydrocolloids, 106*, Article 105839. https://doi.org/10.1016/j.foodhyd.2020.105839

Zhang, T., Sun, R., Ding, M., Li, L., Tao, N., Wang, X., & Zhong, J. (2020). Commercial cold-water fish skin gelatin and bovine bone gelatin: Structural, functional, and emulsion stability differences. *LWT, 125*, Article 109207. https://doi.org/10.1016/j.lwt.2020.109207

Zhang, T., Sun, R., Ding, M., Tao, L., Liu, L., Tao, N., … Zhong, J. (2020). Effect of extraction methods on the structural characteristics, functional properties, and emulsion stabilization ability of Tilapia skin gelatins. *Food Chemistry, 328*, Article 127114. https://doi.org/10.1016/j.foodchem.2020.127114

Zhang, T., Xu, J., Chen, J., Wang, Z., Wang, X., & Zhong, J. (2021). Protein nanoparticles for Pickering emulsions: A comprehensive review on their shapes, preparation methods, and modification methods. *Trends in Food Science & Technology, 113*, 26–41. https://doi.org/10.1016/j.tifs.2021.04.054

Zhang, T., Xu, J., Huang, S., Tao, N., Wang, X., & Zhong, J. (2022). Anhydride structures affect the acylation modification and emulsion stabilization ability of mammalian and fish gelatins. *Food Chemistry, 375*, Article 131882. https://doi.org/10.1016/j.foodchem.2021.131882

Zhang, T., Xu, J., Zhang, Y., Wang, X., Lorenzo, J. M., & Zhong, J. (2020). Gelatins as emulsifiers for oil-in-water emulsions: Extraction, chemical composition, molecular structure, and molecular modification. *Trends in Food Science & Technology, 106*, 113–131. https://doi.org/10.1016/j.tifs.2020.10.005

Zhang, X., Li, Z., Yang, P., Duan, G., Liu, X., Gu, Z., & Li, Y. (2021). Polyphenol scaffolds in tissue engineering. *Materials Horizons, 8*, 145–167. https://doi.org/10.1039/D0MH01317J